

# Benefits of coupling a high-speed laser ablation system to Quadrupole Inductively Coupled Plasma Mass Spectrometry (ICP-MS)

John E Schmelzel, Dhinesh Asogan, Marcus Manecki and Sabrina Antonio, Thermo Fisher Scientific, 355 River Oaks Parkway, San Jose, CA 95134, USA

## ABSTRACT

**Purpose:** Demonstrate the capabilities and limitations of the combination of a new laser-ablation system dedicated to high-speed mapping with quadrupole based ICP-MS systems.

**Methods:** A Teledyne Photon Machines Iridia Laser Ablation System fitted with a Cobalt low-dispersion ablation chamber was directly coupled with a Thermo Scientific™ iCAP™ TQ ICP-MS. Data was acquired using Thermo Scientific™ Qtegra™ Intelligent Scientific Data Solution™ (ISDS) Software and processed using Teledyne Photon Machines HDIP Mass Spectrometry Data Analysis Software.

**Results:** A granite thick section (Shap granite) containing a range of elements in localized crystal distributions was analyzed to demonstrate the ease of coupling to a commercially available high-speed mapping laser ablation system, ease of dwell-time optimization for best signal-to-background ratio and image contrast across all scanned elements, and finally fast analysis times from sampling to image.

## INTRODUCTION

Laser Ablation (LA) coupled with ICP-MS is a well-established way to directly analyze solid samples. The main advantages of laser ablation include the ability to avoid lengthy and potentially contamination-prone sample preparation protocols and the ability to obtain information about the spatial resolution of an analyte in a sample.

The interest in so-called mapping techniques has increased in recent years, calling for laser ablation systems to develop methods to improve sample transfer and therefore speed of mapping experiments. New laser-ablation systems dedicated to high-speed mapping are commercially available and can be easily coupled to quadrupole ICP-MS for such applications.

With the improvement in sample transfer and washout times from laser ablation systems, the time available to analyze discrete packets of sample from a laser pulse is drastically reduced. The limit for lateral resolution using a sequential ICP-MS, such as a quadrupole ICP-MS, is dependent on the dwell times chosen for each measured m/z channel. This has a direct impact on the signal-to-background ratio achievable for each m/z channel; therefore, a direct impact on the final image contrast for each mapped m/z channel.

## MATERIALS AND METHODS

### Sample Preparation

A thick section of Shap Granite was used in this study, mounted in a standard 1 in. round mount. Shap is a coarse-grained granite with large crystals of orthoclase feldspar minerals, and typically comprises biotite, quartz and two types of feldspar (plagioclase and K-feldspar).

### Instrumentation

The choice of appropriate method settings (e.g. triple quad vs. single quad operation, reactive gas used and product ions to be analyzed in Q3) was accomplished using the Reaction Finder method development assistant in the Qtegra ISDS Software. Reaction Finder selects optimum analysis conditions despite the many available options inherent when using a triple quadrupole ICP-MS, but also leaves flexibility for testing different settings for a particular analyte.

Intelligent Mass Selection (IMS) was used on Q1 in all analyses to efficiently remove other ions potentially interfering on the product ion mass whilst maintaining highest detection sensitivity.

Method settings are summarized in Table 1.

Table 1. Instrument Configuration and Operating Parameters

| iCAP TQ ICP-MS Parameters               |   |
|---|---|
| Injector                                | 2.0 mm i.d., quartz   |
| Interface                               | Ni Cones using a High Sensitivity (2.8 mm) Skimmer Insert   |
| RF Power                                | 1300 W  |
| Make-Up Flow                            | 0.66 L·min <sup>-1</sup>  |
| CRC Flow                                | 0.320 mL min <sup>-1</sup> O <sub>2</sub>   |
| Teledyne CETAC Iridia Excimer LA System |   |
| Total Cell Flow                         | Cobalt Cell Flow: 0.30 L min <sup>-1</sup><br>Cup Flow (Long Pulse configuration): 0.45 L min <sup>-1</sup> |
| Spot Size                               | 3 µm  |
| Scan Type                               | Area Scan   |
| Laser Energy                            | ~3.0 J·cm <sup>-2</sup>   |
| Repetition Rate                         | 143 Hz  |
| Dosage / Scan Rate                      | 5 / 85.80 µm sec <sup>-1</sup>  |

### Data Analysis

Data acquisition was accomplished using Qtegra ISDS Software, whilst washout optimization, dwell time optimization and image generation was accomplished using HDIP Mass Spectrometry Data Analysis Software.

## RESULTS AND DISCUSSIONS

### Washout Optimization

For low-dispersion laser ablation set-ups, it is vitally important to assess the washout performance and peak shape of the laser pulses to determine the maximum scanning rate that can be used for a particular number of m/z channels without introducing blurring effects. This can be performed online or between HDIP and Qtegra ISDS using the LA-Monitor module. Here, HDIP can "watch" a folder on the computer and load a csv export generated from Qtegra ISDS software on a per sample basis using the "Automatic Export" function. This can be used to tune the gas flows for the Cobalt Cell flows and the make-up gas flow (see Figure 1 and Figure 2).

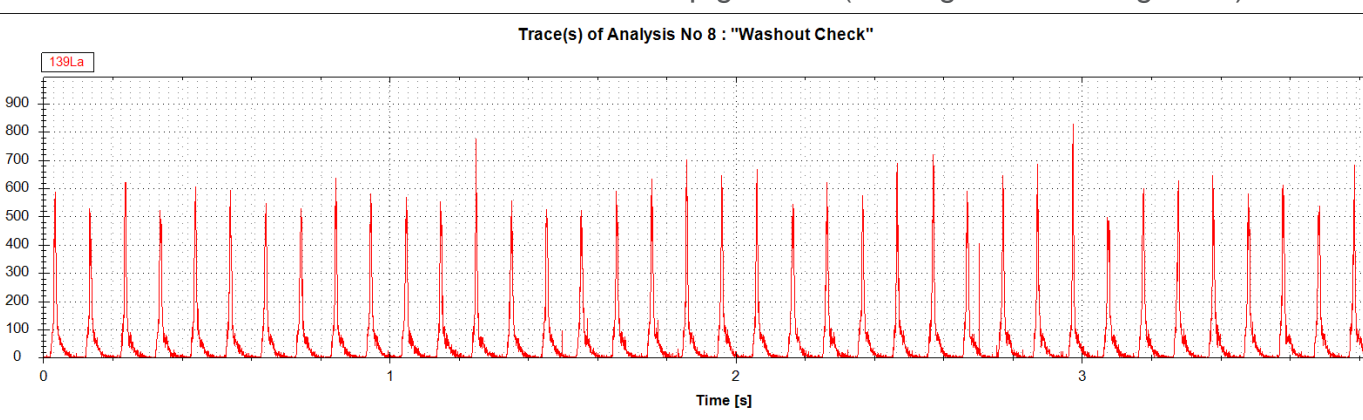


Figure 1. Example Washout Optimization trace from Qtegra ISDS

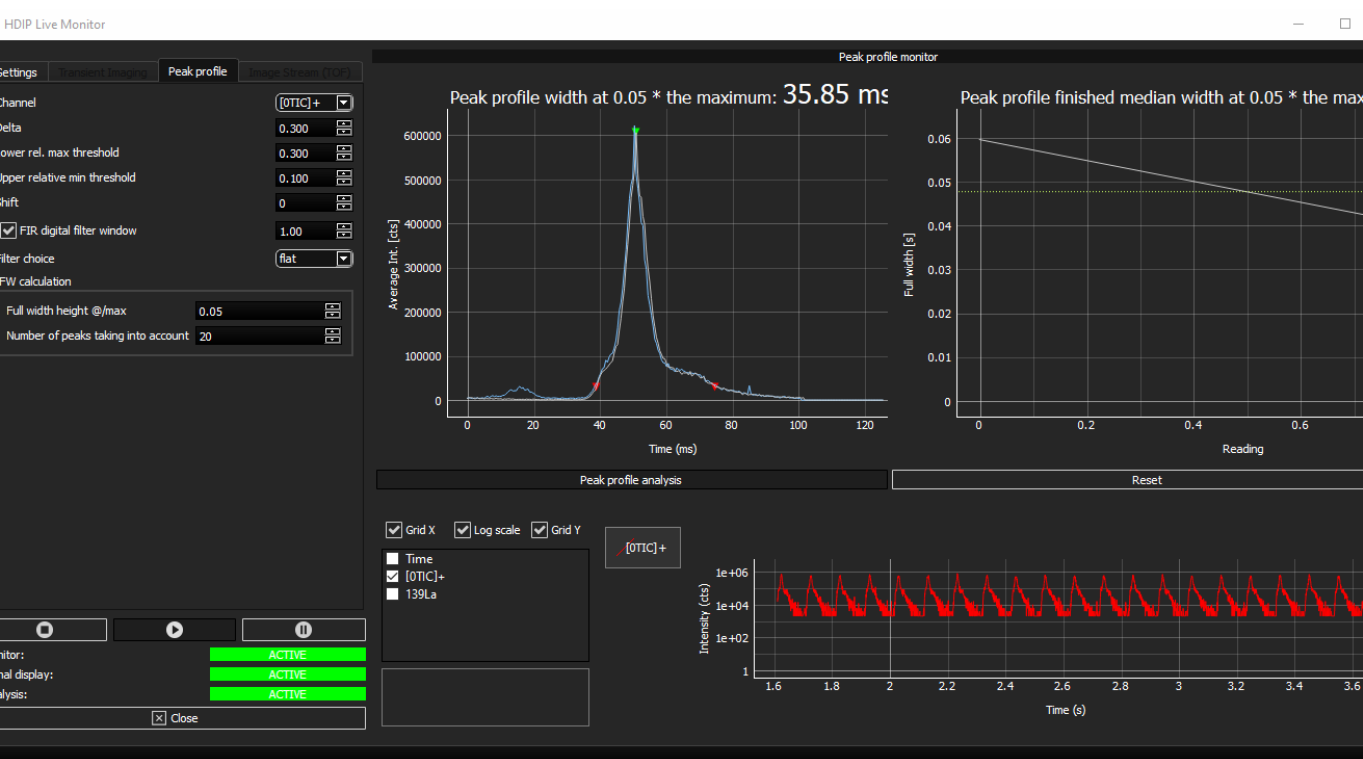


Figure 2. Online Washout Optimization using HDIP

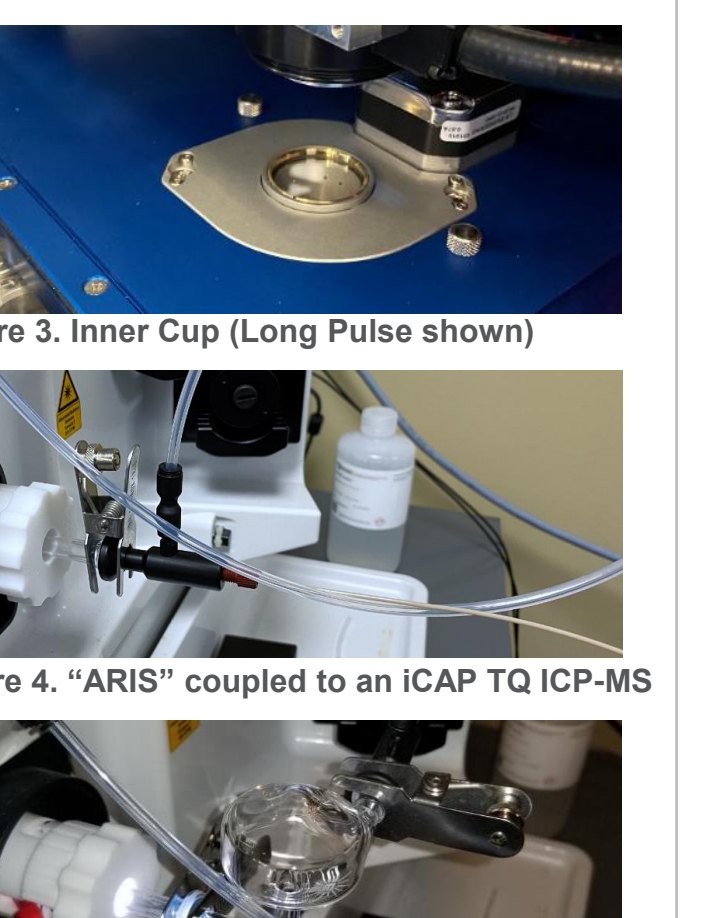


Figure 3. Inner Cup (Long Pulse shown)



Figure 4. "ARIS" coupled to an iCAP TQ ICP-MS



Figure 5. Non-cyclonic Adapter (90 – 150 ms)



Figure 6. Cyclonic Adapter (900 – 2500 ms)

Data acquisition was accomplished using Qtegra ISDS Software, whilst washout optimization, dwell time optimization and image generation was accomplished using HDIP Mass Spectrometry Data Analysis Software.

### Dwell Time and Laser Parameter Optimization

Multi-elemental image generation typically suffers from artefacts inherent in the technique that can be minimized through proper optimization. The main artefacts that contribute to poor 2D image quality are aliasing, blurring (pixelation and smear) and contrast.<sup>1-4</sup>

Aliasing occurs, in essence, if the repetition rate and the cycle time of the laser ablation system and the ICP-MS system are not properly synchronized. This phenomenon causes periodicity in signal intensities that appear as bands in the final image. To combat this, the laser repetition rate and the sampling cycle frequency need to be matched so that an integer number of laser pulses fall within one quadrupole sweep.<sup>1</sup>

Pixelation blur is mainly a factor of the resolution at which the image is gathered, i.e., the laser spot size and the resulting pixel size.<sup>2</sup> To achieve high resolution (low blur), a small spot size must be used; however, this will directly decrease the signal-to-background ratio (i.e., contrast) and increase the total experiment time. The amount of acceptable blurring must therefore be balanced with the desired contrast and experiment time

Smearing, or motion blur, occurs when the transfer of material (washout) cannot keep up with the tracking of the laser across the sample surface (i.e., the scanning rate of the translation stages) and subsequent laser pulses are partially mixed. This is mitigated by adjusting the laser scanning time and repetition rates so that each laser pulse is fully resolved from each other when reaching the detector of the ICP-MS.

Contrast, as discussed briefly above, is a function of signal-to-background ratio and can be adjusted by the amount of material ablated per shot (spot size and/or fluence) or the dwell time of each scanned m/z channel during the quadrupole sweep. Given a set of lasing conditions, optimizing the distribution of dwell times between all m/z channels scanned will achieve the best possible contrast for all analytes in one run.

HDIP contains a module that allows the user to optimize lasing conditions and ICP-MS m/z dwell times to produce high quality images. Given a fixed set of ICP-MS and LA system conditions and the measured washout of the transfer system, the user can import a single line scan across the sample surface to the "LA-Optimize" module, and the software will suggest optimized dwell times for the imaging run and give the user a preview of the resolution and contrast achievable with those laser settings.



Figure 7. Single Line Scan (above) and HDIP "LA-Optimize" module output (below), showing laser conditions and ICP-MS dwell times, and a preview of expected image quality of each m/z channel.

Table 2. Optimized Dwell Times for Final Imaging Run. Since Ca is has relatively low abundance in the sample, most of the quadrupole sweep time is spent on the 44Ca.16O channel to ensure sufficient contrast in the final image. Optimized laser conditions are shown in Table 1.

|                | 39K   39K | 44Ca   44Ca.16O | 56Fe   56Fe | 85Rb   85Rb | 88Sr   88Sr.16O |
|----------------|-----------|-----------------|-------------|-------------|-----------------|
| Dwell Time [s] | 0.0005    | 0.0197          | 0.0005      | 0.0005      | 0.0070          |

Fraction [%]

1.77 69.86 1.77 1.77 24.82

### Shap Granite Images

The following images were generated using an area scan measuring approximately 500 × 800 µm. At a scan rate of 85.8 µm/sec, the entire map was collected in just over 25 minutes.

The mineralogy of Shap granite is mainly plagioclases, K-feldspars, biotite and quartz, with minor inclusions of fluoroapatite, ilmenite and titanite.

Feldspars in general are aluminosilicates with varying amounts of alkali metals. K-feldspars are predominantly potassium enriched, whereas the plagioclase feldspar series contains varying amounts of sodium (as albite) and calcium (as anorthite).

Biotites are a group of black micas, predominantly potassium aluminosilicate enriched with Fe (as annite) to magnesium (as phlogopite). Micas typically also contain Rb and can be used for confirmation.

Quartz is pure SiO<sub>2</sub>; therefore, the absence of major matrix elements indicates its position in the mapped area. It makes little sense to scan for Si given all minerals in granite contain silica.

In the following maps, K, Fe and Rb map to the region dominated by the large black crystal, indicating biotite. Ca is mapped to small regions that indicate plagioclase feldspar, and the remaining area is quartz. The Ca and Sr co-map weakly, with the remainder of Sr in the quartz area. The multi-channel map shows the three phases clearly resolved from each other.

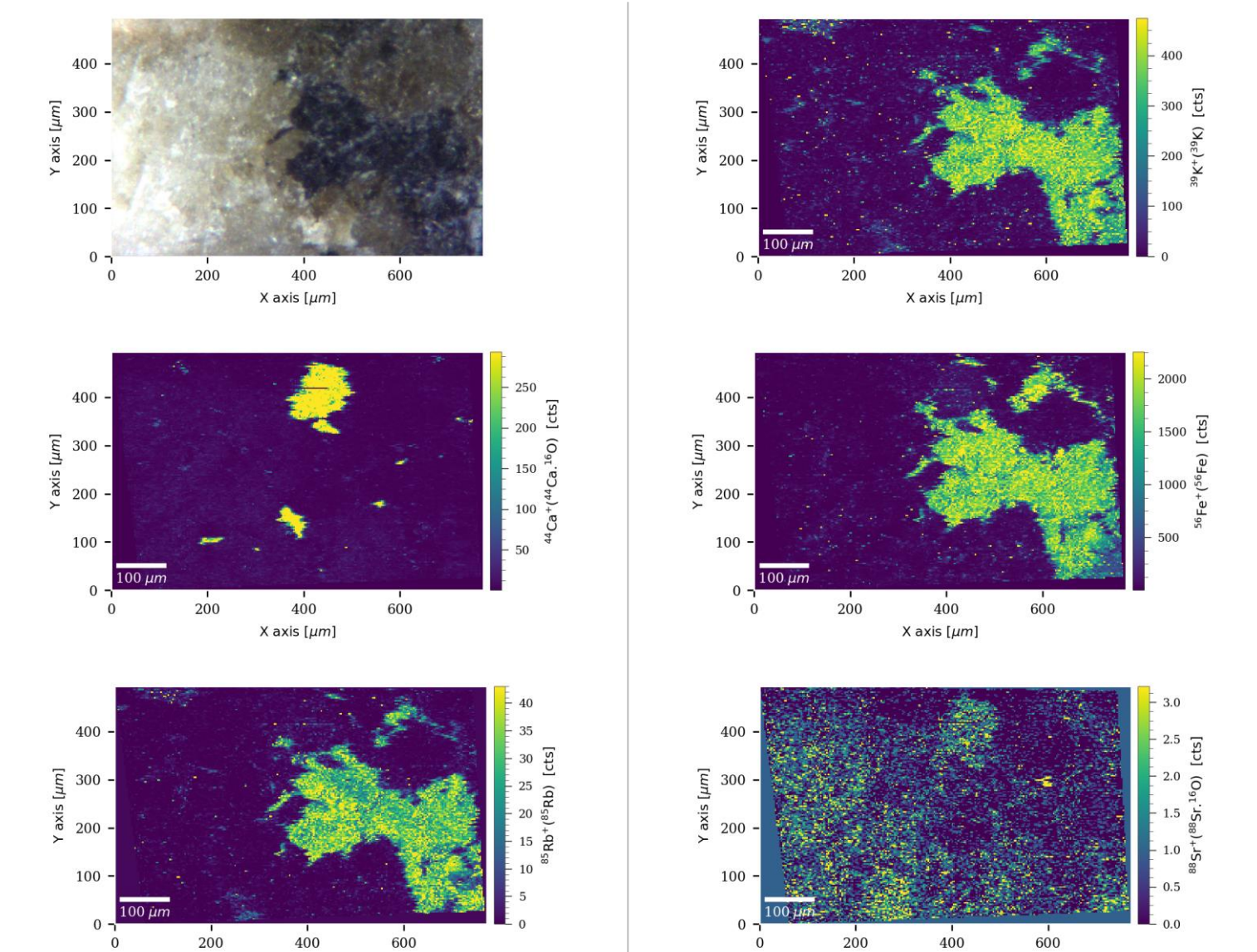


Figure 8. Single element maps of various elements in Shap granite.

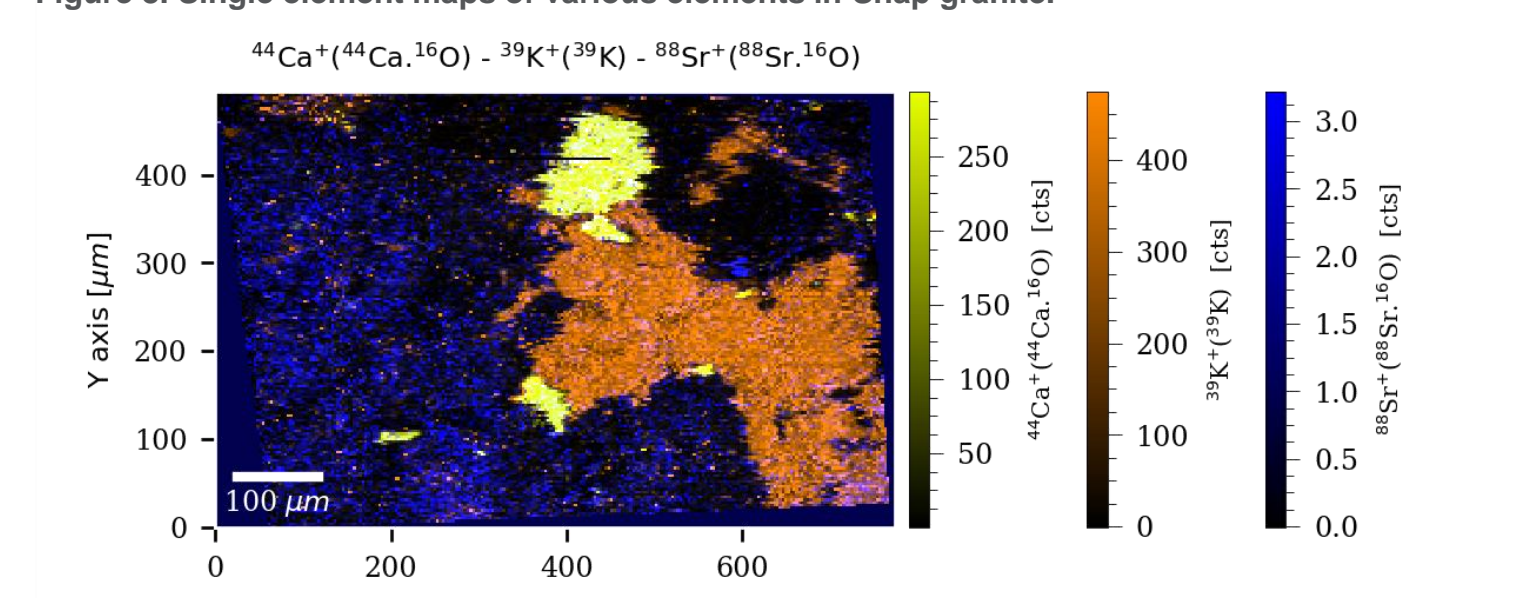


Figure 9. Three element map showing the locations of feldspar (Ca), biotite (K) and quartz (Sr) in the mapped area of Shap granite.

## CONCLUSIONS

Through careful optimization of laser ablation and ICP-MS parameters, it is possible to generate high quality multi-elemental images at a fast rate. The use of new low-dispersion laser ablation cells and aerosol transfer technology is not limited to simultaneous mass spectrometers and is also applicable to sequential scanning mass spectrometers such as Quadrupole ICP-MS.

The major limitation of coupling low-dispersion Laser Ablation systems to sequential mass spectrometers is the limited number of elements that can be scanned; however, this is offset by the sensitivity and the specificity of, especially, triple quadrupole ICP-MS systems for the reduction of interferences on select analytes.

Most imaging experiments can be reduced to three or four analytes of interest, and in these cases LA-ICP-MS coupled to Triple Quadrupole ICP-MS using a low-dispersion, fast imaging setup can provide the analytical data quality required to answer challenging research questions.

## REFERENCES

1. S. J. M. Van Malderen et al., *Spectrochim. Acta, Part B*, 2018, 140, 29-34
2. J. T. van Elteren et al., *J. Anal. Atom. Spectrom.*, 2019, 34, 1919-1931
3. J. T. van Elteren et al., *J. Anal. Atom. Spectrom.*, 2020, 35, 2494-2497
4. M. Šala et al., *J. Anal. Atom. Spectrom.*, 2021, 36, 75-79

## TRADEMARKS/LICENSING

© 2021 Thermo Fisher Scientific Inc. All rights reserved. Teledyne Photon Machines and Teledyne CETAC Technologies are brands of Teledyne Instruments Inc. All trademarks are the property of Thermo Fisher Scientific and its subsidiaries. This information is not intended to encourage use of these products in any manner that might infringe the intellectual property rights of others.



thermo scientific